**Neuroendocrine Control of Intestinal Regeneration Through the Vascular Niche in *Drosophila*.**

**André B. Medina[1,3], Jessica Perochon[2], Cai Johnson[2], Yuanliangzi Tian[2], Karen Bellec[2], Yachuan Yu[1] and Julia B. Cordero[1,2*]**

[1] CRUK Scotland Institute. Institute of Cancer Sciences. University of Glasgow. Garscube Estate, Switchback Road, G61 1BD. Glasgow, U.K.

[2] Wolfson Wohl Cancer Research Centre. Institute of Cancer Sciences. University of Glasgow. Garscube Estate, Switchback Road, G61 1QH. Glasgow, U.K.

[3] Present address: Charité Medical University Berlin.13353 Berlin, Germany.

* Corresponding author: julia.cordero@glasgow.ac.uk

Keywords: Trachea, neurons, enteroendocrine cells, intestinal regeneration, Dh31, PDGF/VGEF, interorgan signaling.

**Abstract**

Robust and controlled intestinal regeneration is essential for the preservation of organismal health and wellbeing and involves reciprocal interactions between the intestinal epithelium and its microenvironment. While knowledge of regulatory roles of the microenvironment on the intestine is vast, how distinct perturbations within the intestinal epithelium may influence tailored responses from the microenvironment, remains understudied. Here, we present previously unknown signaling between enteroendocrine cells, vasculature-like trachea, and neurons, which drives regional and global stem cell proliferation during adult intestinal regeneration in *Drosophila*.

Injury-induced ROS from midgut epithelial cells promotes the production and secretion of Dh31, the homolog of mammalian Calcitonin Gene-Related Peptide (CGRP), from anterior midgut EE cells. Dh31 from EE cells and neurons signal to Dh31 receptor within TTCs leading to cell autonomous production of the vascular endothelial growth factor (VEGF) and platelet-derived growth factor (PDGF)-like Pvf1. Tracheal derived Pvf1 induces remodeling of the tracheal stem cell niche and regenerative ISC proliferation through autocrine and paracrine Pvr/MAPK signalling, respectively. Interestingly, while EE Dh31 exerts broad control of ISC proliferation throughout the midgut, functions of the neuronal source of the ligand appear restricted to the posterior midgut. Altogether, our work has led to the discovery of a novel enteroendocrine/neuronal/vascular signaling network controlling global and domain specific ISC proliferation during adult intestinal regeneration.

## Introduction

The high regenerative nature of the intestinal epithelium, which is essential for organismal wellbeing, relies on the tight coordination of interdependent stem cell intrinsic processes and multicellular paracrine signals (Hageman et al., 2020, Zhou and Boutros, 2023). Consistently, research on intestinal regeneration requires in vivo model systems that account for the complex inter-cellular and inter-tissue signaling between the gut epithelium in its natural microenvironment. Due its physiological sophistication, vast single cell molecular information and richness of tools for spatially and temporally restricted genetic manipulations, the fruit fly *Drosophila melanogaster* has been an excellent in vivo model system for the study of multi-organ communication in the intestine (Medina et al., 2022).

Akin to the mammalian intestine, the adult *Drosophila* midgut regenerates through the action of stem cells (Micchelli and Perrimon, 2005, Ohlstein and Spradling, 2005) operating under the control of signals emerging from a rich microenvironment, collectively referred to as the intestinal stem cell (ISC) niche (Jiang et al., 2011, Jiang et al., 2009a, Amcheslavsky et al., 2014). In the mammalian gastrointestinal tract, diverse cellular types, including intestinal epithelium resident cells and cells from the associated mesenchyme provide physical support, contractility, oxygen, and multiple stem cell niche factors such as Wnts, BMP, EGFs and R-Spondin, which instruct ISC self-renewal in homeostatic and challenging conditions (Kim et al., 2020, McCarthy et al., 2020, Stzepourginski et al., 2017, Niec et al., 2022).

In addition to ISCs, the fly midgut epithelium consists of two subtypes of undifferentiated stem cell progeny, namely, enteroblasts (EBs) and pre-enteroendocrine cells, which are precursors of absorptive enterocytes (ECs) and secretory enteroendocrine cells (EEs), respectively (Chen et al., 2018). As in mammals, cells within the fly midgut epithelium and gut associated tissues, such as the visceral muscle (VM), terminal tracheal cells (TTCs) and enteric neurons (ENs) are components of the intestinal microenvironment that contribute to robust ISC proliferation and differentiation as part of a complete intestinal regeneration program (Medina et al., 2022, Petsakou et al., 2023).

A large body of research and cutting-edge technology has led to the discovery of the multiple components of the intestinal microenvironment and the myriad of stem

cell niche factors they produce to instruct ISC function during tissue regeneration (Hageman et al., 2020, Kim et al., 2020, Harnack et al., 2019). However, less is known about how local and/or challenge-specific changes within the intestinal epithelium might influence the intestinal microenvironment to achieve robust and regenerative responses of the intestine, tailored to the environmental demands.

Secretory EE cells within the *Drosophila* and mouse intestine are a highly, diverse, specialized and compartmentalized progeny of ISCs with the ability to sense a wide range of cues for within the intestine and the external environment (Guo et al., 2019, Gehart et al., 2019, Beumer et al., 2020, Lebrun et al., 2017). Signals received by EE cells are translated into the production of peptide hormones acting at short range, in an autocrine or paracrine fashion, or in a more classical endocrine or systemic mode, via their release into the circulation (Gribble and Reimann, 2016, Guo et al., 2022). The molecular and functional versatility of EE cells make them likely candidates to endow the gut with a highly refined regenerative response to the diversity of challenges faced by the intestinal epithelium. While nutrient regulated response of EE cells and their constitutive function in the maintenance of intestinal homeostasis and growth has been recognized for decades (Scopelliti et al., 2014, Amcheslavsky et al., 2014, Martin et al., 2005, Drucker et al., 1996, Sasaki et al., 2001, Lin et al., 2022), little is understood about the regulation and function of EE cells in intestinal regeneration. Recent datasets and publicly available toolkits for in situ gene expression analysis and independent genetic manipulation of EE peptide hormones and their cognate receptors, open a door for new and fundamental discoveries on the communication between EE cells and the intestinal microenvironment (Hung et al., 2020, Li et al., 2022, Liu et al., 2022b).

Here, we uncover multi-tissue signalling crosstalk between intestinal EE cells, gut associated vascular-like trachea and neurons, involving Calcitonin Gene-Related Peptide and PDGF/VEGF like factors to control global and domain specific intestinal regeneration in *Drosophila*.

## Results

### Intestinal damage promotes an evolutionary conserved increase in enteroendocrine cells

Damage-induce repair of highly regenerative tissues, such as the intestine, include increased epithelial cell death and compensatory stem cell proliferation, resulting in significant changes in cellular dynamics in *Drosophila* (Amcheslavsky et al., 2009, Jiang et al., 2009b, He et al., 2018) and higher organisms (Parikh et al., 2019). Alterations in enteroendocrine (EE) cells are recognised features of intestinal damage (Dahly et al., 2003, Lebrun et al., 2017, Martin et al., 2005), pathogenic infection (Yang et al., 1990, Forbes et al., 2009, Bosi et al., 2005, Ovington, 1985, van Marle et al., 2013) and inflammatory bowel disease (IBD) (Worthington et al., 2018, Harrison et al., 2013). However, the aetiology and functional implications EE cell changes to adult intestinal health and disease, remain largely unknown.

We analysed the proportion of EE cells in adult *Drosophila* midguts by staining with an antibody against the transcription factor, Prospero (Pros), and observed that damage to the midgut epithelium caused by oral feeding with the entomopathogen *Pseudomonas entomophila* (*Pe*), the DNA-damage agent bleomycin or the basal membrane disruptor dextran sodium sulphate (DSS), caused a significant increase in Pros positive cells (Figure 1A, 1B). Mouse intestinal samples from animals subject to DNA damage by whole body irradiation, or with inflammatory colitis induced by treatment with DSS also showed a noticeable increase in the number of Chromogranin A (ChgA) positive EE cells in the colon (Figure 1C, 1C') and small intestine (Figure 1C''). Taken together, our results suggest that increased EE cell proportion is a conserved feature of *Drosophila* and mouse intestines undergoing acute damage, which recapitulate manifestations of related human intestinal perturbations (Sciola et al., 2009, Zissimopoulos et al., 2014, Zhang et al., 2019). Next, we used *Drosophila* to investigate the nature of such EE phenotype and its functional significance to the intestinal response to damage.

### Regulation of the EE-cell derived peptide hormone Dh31 is required to fulfill the regenerative capacity of the midgut epithelium upon damage

EE cells secrete peptide hormones that are constitutively required for the maintenance of ISC homeostasis and tissue growth in both fruit flies (Scopelliti et al.,

2014, Amcheslavsky et al., 2014) and mammals (Drucker et al., 1996, Sasaki et al., 2001). However, the wide diversity and exquisite regionalization of EE cells in the gastrointestinal track (Beumer et al., 2020, Guo et al., 2019, Gehart et al., 2019) strongly suggest the potential for specialized and regulated responses of these cells. We therefore asked whether the global increase in EE cell numbers observed in damaged intestines may reflect on an EE cell sub-type specific response and/or function in tissue regeneration. We performed an RNA interference (RNAi) mini-screen to knockdown 9 different peptide hormones produced by EE cells using the temperature sensitive driver *voilà-Gal4*$^{ts}$, which labels all EEs in the midgut (Scopelliti et al., 2014). We measured intestinal regeneration by counting the number of proliferative ISCs (PH3 positive) within the posterior midgut of mated females fed overnight with the pathogen *Pe*. We observed that knocking down the expression of *Dh31* caused the strongest and most consistent reduction in PH3 positive cells (Figure S1A, S1B), suggesting a preferential role for Dh31 producing EE cells in intestinal regeneration. Whole body *Dh31* loss of function and further EE cell gene knockdown using two RNAi lines (*Dh31-IR1* and *Dh31-IR2*) confirmed our initial observations that *Dh31* is required for intestinal regeneration (Figure 1D, 1E). Similarly, knocking down *Dh31* in Dh31 expressing cells (*Dh31-Gal4*$^{ts}$) in animals subject to intestinal damage by oral administration of *Pe*, bleomycin or DSS, resulted in significantly reduced regenerative ISC proliferation (Figure 1F, 1G and 1H).

Due to the neuroepithelial characteristics of EE cells, peptide hormones secreted by EE cells are also produced in the brain and genetic drivers targeting this cell population, including *voilà-Gal4* and *Dh31-Gal4* are expressed both in the midgut and neurons (Scopelliti et al., 2014, Lin et al., 2022). To address EE specific functions of Dh31, we screened for a combination of genetic tools that would reduce *Gal4* expression and therefore impair gene targeting within neurons, while allowing gene manipulations in EE cells. We found that a cholinergic line, *ChAT-Gal80* (Kitamoto, 2002) could strongly decrease neuronal GFP expression driven by *voila-Gal4*, with no effect in the midgut. Importantly, while a significant reduction of *Dh31* expression was observed in *voilà*$^{ts}$ driven RNAi, *Dh31* knockdown with *voilà*$^{ts}$*,ChAT-Gal80* did not affect *gene* expression levels in the brain, (Figure 1I). Consistently, we observed no reduction in Dh31 immunostaining in either the brain or ventral nerve cord (VNC) of *voilà*$^{ts}$*,ChAT-Gal80>Dh31-IR* animals, while midgut protein signal was undetectable

(Figure 1J, S1C). Importantly, gut specific *Dh31* knockdown was sufficient to impair regeneration in damaged midguts as revealed by reduced ISC proliferation in the anterior and posterior midgut (Figure 1K). Overexpression of *Dh31* or activation of Dh31$^+$ EE cells through expression of the mammalian capsaicin receptor (VR1) was not sufficient to promote ISC proliferation in homeostatic conditions (Figure S1D, S1E). We noted that, in addition to EE cells, Dh31 is expressed in a subset of enteric neurons innervating the hindgut and posterior midgut (Cognigni et al., 2011) (Figure S1F). Interestingly, neuronal specific knockdown of *Dh31* using *nSyb-gal4* (*nSyb$^{ts}$*) (Figure S1G) resulted in reduced regenerative ISC proliferation, which was restricted to the posterior midgut (Figure S1H). Altogether, these results indicate that EE cell derived Dh31 is necessary for global damage induced regeneration of the adult *Drosophila* midgut. An additional source of the neuropeptide, produced by neurons, contributes locally to posterior midgut regeneration.

**Dh31 production is regulated by intestinal damage**

We next assessed the distribution of Dh31$^+$ EE cells in the midgut using a *Dh31-Gal4>mCD8-GFP* gene expression reporter and an antiserum against Dh31 protein. Similar to previous reports (Veenstra et al., 2008, Benguettat et al., 2018), high levels of Dh31 immune-labelling and reporter expression in posterior midgut regions R4c and R5, and a low number of cells with weaker protein and gene expression signal in the rest of the homeostatic midgut (Figure 2A-C and S2A). On the other hand, local infectious challenge to the intestinal epithelium with *Pe*, resulted in a strong increase in immuno-labelling of Dh31$^+$ EE cells and gene expression in the anterior midgut (Figure 2B, C), a slight decrease in EE cell immunostaining in the posterior midgut (Figure 2B' and 2C'). We observed no clear pattern of regulation of Dh31 levels in enteric neurons (Figure S2F). Quantification of *Dh31* transcription by qRT-PCR showed a consistent increase in mRNA levels, specifically in the anterior midgut with no change detected in the posterior compartment (Figure 2D). Altogether, these results suggest domain specific regulation of *Dh31* mRNA and protein in response to pathogenic damage, which is restricted to the anterior midgut.

EE cells store peptide hormones into vesicles and secrete them locally or systemically into the haemolymph following activation by specific stimuli in a process that involves increase in intracellular Calcium ($Ca^{2+}$) (Scopelliti et al., 2018, Lin et al.,

2022). To further interrogate the nature of upregulated Dh31 upon midgut damage (Figure 2A-3D), as to whether this may reflect increased peptide retention or higher peptide production and secretion, we measured Dh31$^+$ EE cell activity *ex vivo* by accessing cytoplasmic $Ca^{2+}$ levels through the use of GCaMP7, a genetically encoded calcium sensor. We expressed GCaMP7 in Dh31$^+$ EE cells after different periods of 5% sucrose or *Pe* feeding. We detected increased Dh31$^+$ cell activity in the anterior midgut as soon as 4h of infection, which remained consistently high after 8h and 16h of infection (Figure 2E and 2F). Co-expression of GCaMP7 and the nuclear reporter RedStinger, using a *Dh31* knock-in *Gal4* line *Dh31-T2A-Gal4*, showed that almost all Dh31$^+$ EE cells were activated in the anterior midgut after 16h of *Pe* infection when compared to sucrose fed animals (Figure S2B) We did not detect any evident changes in basal levels $Ca^{2+}$ signal in Dh31$^+$ EE cells within the posterior midgut, which remained constitutively high regardless of treatment (Figure 2G). Taken together, our results demonstrate inducible production and secretion of Dh31 from EE cells in the anterior midgut compartment upon pathogen induced damage of the adult *Drosophila* intestinal epithelium.

**Gut epithelial derived reactive oxygen species induce Dh31 production in *Drosophila*.**

Intestinal damage triggered by pathogenic bacteria infection generates high levels of reactive oxygen species (ROS) in the gut lumen, mainly via enterocytes (ECs) as a protective mechanism from the host against the pathogen (Morris and Jasper, 2021). Dh31$^+$ EE cells in the anterior midgut of developing animals are responsive to extracellular ROS generated by short-term bacterial infection, consequently promoting the secretion of Dh31, a response needed to induce gut peristalsis and expel pathogens from the intestine (Benguettat et al., 2018). Blocking ROS in the adult midgut by feeding *Pe* infected animals with the antioxidant *N-acetyl cysteine* (NAC) or by genetically inhibiting ROS production in ECs via DUOX knockdown led to a significant reduction in EE cell Dh31 immunolabelling in the anterior midgut (Figure 3A, 3B, 3C and 3D). Furthermore, feeding animals with a sucrose solution containing $H_2O_2$, a form of ROS commonly produced during bacterial infection, increased EE cell Dh31 immunolabelling specifically within the anterior midgut (Figure 3E, 3F) (Figure S3A). Therefore, ROS produced by midgut epithelial cells is necessary and sufficient to induce Dh31 production in EE cells of the anterior midgut.

**Tracheal Dh31 receptor signaling is required for ISC proliferation during midgut regeneration**

To begin to understand how damage-induced Dh31 promotes regeneration, we investigated the expression of the Dh31 receptor (Dh31R). Single cell RNAseq, bulk RNAseq and loss of functional experiments, have previously demonstrated the presence of *Dh31R* in midgut ECs, EEs and the visceral muscle (VM) (Dutta et al., 2015, Benguettat et al., 2018, Hung et al., 2020). We used a *Dh31-R* knock-in *Gal4* reporter, which recapitulates the endogenous expression pattern of the *Dh31-R* gene (Deng et al., 2019), to express GFP (*Dh31-R>GFP)* and therefore visualize receptor expression in situ. We observed GFP in uncharacterised enteric neurons of the crop and anterior midgut, PDF expressing neurons in the posterior midgut, the VM and ECs in the anterior midgut (Figure 4A and S4A) and within terminal trachea cells (TTCs) though out the full length of the midgut (Figure 4B). We next used inducible RNAi lines to knockdown *Dh31R* from various compartments within the midgut and closely associated tissues, including PDF producing neurons (Figure S4B) (*Pdf$^{ts}$>Dh31R-IR1),* visceral muscle (*how$^{ts}$>Dh31R-IR1)*, ECs (*Mex$^{ts}$>Dh31R-IR1)* and in TTCs (*dSRF$^{ts}$>Dh31R-IR1)*. While mild reduction in intestinal regeneration was observed upon *Dh31R* knockdown in the VM and ECs (Figure S4D, S4E), receptor downregulation in TTCs resulted in most robust and consistent impairment of regenerative ISC proliferation throughout the midgut of *Pe* infected animals (Figure 4C, 4D and S4F) or treated with bleomycin (Figure 4E). Therefore, we focused the rest of our work on studying the role of Dh31 regulating intestinal regeneration via signaling through tracheal Dh31R.

**Dh31R signaling affects TTCs remodeling and MAPK activation in the regenerating midgut.**

Adult terminal tracheal cell plasticity and the production of stem cell niche factors by the trachea are essential to support the regenerative function of ISCs following midgut injury (Perochon et al., 2021, Tamamouna et al., 2021). Downregulating *Dh31R* in TTCs (*dSRF$^{ts}$>Dh31R-IR*) led to significantly diminished TTC remodeling in *Pe* infected midguts (Figure 5A, 5B). These results suggest that the activation of Dh31/Dh31R signaling within adult gut trachea and its contribution to midgut regeneration, involves the induction of TTC remodeling. ROS dependent

production the *Drosophila* FGF-like ligand Branchless (Bnl) by the trachea and intestinal epithelium, drives regenerative ISC proliferation through paracrine activation of the FGF receptor Breathless (Btl) and downstream MAPK signaling in ISCs (Perochon et al., 2021, Tamamouna et al., 2021). While we observed significant downregulation of MAPK activation in ISCs of injured midguts with impaired tracheal Dh31R signaling (*dSRF$^{ts}$>Dh31R-IR)* (Figure 5C, 5D), there was no impact on *bnl* upregulation (Figure S5A, S5B). These data suggest that Dh31R dependent tracheal remodeling and MAPK activation in ISCs is unlikely to be mediated by Bnl/Btl signaling.

**Tracheal derived Pvf1 drives midgut regeneration through activation of dual paracrine and autocrine Pvr/MAPK signaling.**

We hypothesized that MAPK activating factors other than Bnl/FGF might be regulated by Dh31R signaling in the trachea. Analysis of our TTC Targeted DamID (TaDa) data (Perochon et al., 2021), revealed significant binding of RNA Pol II to genes encoding for *Drosophila* vascular endothelial growth factor (VEGF) and platelet-derived growth factor (PDGF)-like secreted factors *Pvf1* and *Pvf3 (Parsons and Foley, 2013)* (Figure S5C). Autocrine Pvf/Pvr expression and MAPK signaling activation within stem/progenitor cells of the adult midgut is necessary for ISC proliferation and differentiation in the absence of environmental challenges (Bond and Foley, 2012). We next tested whether paracrine Pvf/Pvr signaling between trachea and the midgut epithelium, respectively, may be involved in the regenerative response of ISCs to pathogenic midgut damage. Firstly, RNAi knockdown of *Pvf1* from TTCs showed that *Pvf1* was necessary to induce ISC proliferation during midgut regeneration (Figure 5E). Complementary, knocking down of *Pvr* in ISCs/EBs using the *escargot-gal4* driver (*esg$^{ts}$>GFP*) led to almost complete impairment of ISC proliferation and MAPK signaling activity within regenerating midguts (Figure 5H, 5I, 5J). Interestingly, unlike tracheal produced Bnl that is redundant for TTC remodeling (Perochon et al., 2021), knocking down *Pvf1* from TTC (*dSRF$^{ts}$>GFP, Pvf1-IR1)* led to significant impairment of tracheal remodeling in *Pe* infected midguts (Figure 5F, 5G). These results suggest that, in addition to signaling paracrinally to ISC expressing Pvr, Pvf1 may also impact ISC proliferation indirectly, by autocrine signaling through its receptor expressed within the trachea. Consistently, trachea specific knock down of *Pvr* impairs TTC remodeling inhibits ISC proliferation in regenerating midguts (Figure S5D, S5E, S5F). Altogether,

our results uncover a new cellular source and dual signaling mode for the *Drosophila* VEGF/PDGF-like ligand, Pvf1, regulating midgut regeneration from the tracheal stem cell niche and via ISC and TTC receptors. These versatile characteristic of Pvf1 also make it a likely candidate for regulation by Dh31/Dh31R signaling in TTCs in the regenerating midgut.

**Dh31R signaling regulates tracheal Pvf1 production in the regenerating midgut**

To investigate a potential connection between Dh31/Dh31R signaling and Pvf1, we stained *Dh31R-T2A-Gal4>mCD8-GFP* midguts carrying endogenously tagged Pvf1 (Pvf1-HA) with an anti-HA antibody (Figure 6A), which revealed co-localization between the two. Immunostaining to detect either HA-tagged or unmodified PVF1 revealed strong upregulation of PVF1 in ECs and TTCs of *Pe* treated midguts (Figure S6A). Importantly, knocking down *Dh31R* from trachea (Figure 6B, 6C) or *Dh31* from neurons (Figure 6D, 6E) also impaired Pvf1 upregulation in TTCs of the posterior midgut

Tracheal remodeling and increased EE cell Dh31 expression are highly dependent on damage-induced ROS production from the midgut epithelium (Perochon et al., 2021) (Figure 3), we therefore asked whether Pvf1 was also regulated by ROS. Indeed, Pvf1 upregulation was almost completely prevented in *Pe* treated animals fed with the antioxidant NAC (Figure 6F, 6G). Altogether, our results uncover a novel EE/Neuronal/tracheal signaling network controlling global and domain specific ISC proliferation during adult midgut regeneration. Mechanistically, this interorgan signaling system involves regulated production of Dh31 by EE cells in the anterior midgut and constitutive sourced of the ligand from EE cells in the posterior midgut and neurons. Dh31 signaling to Dh31R within TTCs induces the production of a previously uncharacterized source of Pvf1 from the trachea. Reciprocally, tracheal Pvf1 induces tracheal remodeling and regenerative ISC proliferation through autocrine and paracrine Pvr/MAPK activation, respectively (Figure S6B).

## Discussion

### Dh31 and EE cells in intestinal regeneration

Our study provides new evidence of complex fine-tuning of intestinal regeneration trough mutli-tissue signaling and the importance of damage dependent regulation of EE cell function and specific peptide hormone secretion in this process. Although EEs have been previously shown to contribute to intestinal homeostasis in flies and mammals (Amcheslavsky et al., 2014, Scopelliti et al., 2014, Drucker et al., 1996, Sasaki et al., 2001), our work represents the first report of EE and neuronal derived peptide hormone and PDGF/VEGF vascular signalling during intestinal regeneration.

Interestingly, although Dh31 contributes to ISC proliferation in the anterior region, we noticed stronger effects of the peptide in the posterior midgut, where we also observed neuronal peptide expression and an impact of Dh31 on TTCs remodelling and PVF1 regulation. We envision different possibilities to explain these observations. Dh31 acts in the midgut may not only paracrinally but also via its release into the circulation, targeting its receptor in regions of the midgut far away from where it is produced. In fact, Dh31 has been previously reported to act systemically via secretion into the haemolymph (Lin et al., 2022). Alternatively, the 3D conformation of the midgut brings the anterior and posterior regions into close proximity (Buchon et al., 2013) and could therefore facility the communication between cells across gut sections. In a pathogenic infection context, a broader secretion and action of Dh31 from the anterior midgut, which is the first to sense opportunistic bacteria via ROS, could be beneficial as it transmits the signal to the posterior midgut in a faster way. A similar observation was described by other studies in which Dh31 from the anterior midgut of developing larvae was necessary and sufficient to promote intestinal contraction via activation of Dh31-R in the visceral muscle to eliminate opportunistic bacteria (Benguettat et al., 2018). Similarly, such study reported that although only Dh31 from the anterior midgut was responsive to ROS, intestinal contractility also happened strongly in the posterior midgut.

Apart from its short-range role within the midgut and midgut associated tissues, Dh31 secretion into the circulation has clear systemic consequences, which we have yet to explore in the context of intestinal damage. EE-derived Dh31 was recently

shown to signal to neurons in the brain altering feeding and courtship behaviour (Lin et al., 2022). Dh31-R is highly expressed in neurons in the brain, ventral nerve cord and corpora allata (Deng et al., 2019, Kurogi et al., 2023). Additionally its isoform Dh31-R RC is widely expressed in the glia (Deng et al., 2019). Therefore, damage induced gut Dh31 may regulate systemic traits, which could in turn be potentially instructive to the process of intestinal regeneration.

We observed here a conserved phenomenon where the proportion of EEs are increased during intestinal injury in both flies and mammals. Similar observations were also found in *Drosophila* in different context of intestinal injury or aging (He et al., 2018, Tauc et al., 2021, Liu et al., 2022a). Given the regenerative role of EEs described here and additional protective and immune roles described in the literature (Benguettat et al., 2018, Kamareddine et al., 2018), increased EE cells might have a protective role and is worth further investigation in mammals.

**Dh31 and its communication with the vascular intestinal stem cell niche**

We show here that Dh31 participates in intestinal regeneration via communication with its receptors in the vascular-like tracheal component of the ISC niche but not by targeting ISCs directly. Interestingly, signal relay to associated tissues is a common mechanism used by peptide hormones in both flies as humans (Scopelliti et al., 2014, Amcheslavsky et al., 2014, Estall and Drucker, 2006, Baldassano and Amato, 2014), as perhaps the most efficient strategy to translate local cues into global tissue responsed. While our results suggest stronger impairment of midgut regeneration when knocking down Dh31 receptor in terminal tracheal cells compared to other niche cells, we cannot rule out a role for Dh31 signlaing to receptor in other midgut associated tissues and epithelial cells, as we observed small but significant role in proliferation when affecting Dh31R expression in such cellular compartments.

In humans, Dh31 has similarities with the Calcitonin gene related peptide (CGRP), which is a splicing variant from the Calcitonin gene (Furuya et al., 2000). Similarly, CGRP have very diverse functions in organismal homeostasis, acting locally or systemically in multiple organs. However, CGRP is not found expressed in EE cells but mainly in immune cells and central and peripheral neurons (Russell et al., 2014). Our evidence on the expression and function of neuronal derived Dh31 is a clear parallel to the latter. Indeed, as we observed here, CGRP communicates with the

cardiovascular system and is known to be a potent vasodilator by activating cAMP pathway through its receptor in endothelial cells and the smooth muscle that surrounds them (Russell et al., 2014). Additionally, CGRP has also been reported to have anti and pro-inflammatory roles and facilitates wound healing possibly by local upregulation of growth factors such as VEGF, FGF, TGF-β (Toda et al., 2008, Mishima et al., 2011). In the intestine, new studies are beginning to show the importance of CGRP in inflammatory contexts (Xu et al., 2019, Manion et al., 2023). However, its CGRP functions in tissue regeneration are largely unexplored and our study provides the first evidence of such a role in the fly midgut, prompting similar investigations in mammals.

## Figure Legends

**Figure 1: EE-cell derived peptide hormone Dh31 is required to fulfill the regenerative capacity of the midgut epithelium upon damage.** (A) Immunofluorescence of EE cells labeled by Pros in the posterior midgut of flies treated with sucrose, *Pe*, Bleomycin or DSS. (B) Quantification of EE cell proportion as in A. (C) Representative images of EE cells, labeled by Chromogranin A (ChgA) immunohistochemistry, in the mouse large intestine (L.I) and small intestine (S.I). Control and whole body irradiation (C') and control and DSS treatment (C'') in the L.I and control and whole body irradiation in the S.I (C'''). (D) Quantification of PH3+ cells in sucrose and Pe treated posterior midguts of Dh31 whole body knockout animals. (E) Quantification of PH3+ cells in sucrose and Pe treated posterior midguts following Dh31 knockdown (*Dh31*-IR1 and *Dh31*-IR2) with voilaG4. (F, G, H) Quantification of PH3+ cells in posterior midguts treated with *Pe* (F), Bleomycin (G) and DSS (H) following *Dh31* knockdown (KD) (*Dh31*-IR1 and/or *Dh31*-IR2) specifically in Dh31+ cells. (I) *Dh31* mRNA expression value in fly heads following *Dh31* KD (*Dh31*-IR2) driven by voilaG4 with ChatG80 or without. (J) Effect on Dh31 protein (green) levels in the brain and posterior midgut following *Dh31* KD (*Dh31*-IR2) with a gut specific driver. Representative confocal images. (K) Quantification of PH3+ cells in the posterior midgut of animals treated with sucrose or *Pe* following Dh31 knockdown (*Dh31*-IR1 and *Dh31*-IR2) specifically in the midgut. (B) Two-tailed unpaired Student's t-test. (I) Ordinary one-way ANOVA and (D, E, F, G, H) Two-way ANOVA followed by Tukey's multiple comparisons test. * (P<0.1) *** (P<0.001) **** (P<0.0001). Scale bar = 50µm.

**Figure 2**: **Dh31 production is regulated by intestinal damage.** (A) Schematic view of Dh31 expression pattern in the midgut. (B) Expression levels of Dh31 detected by immunostaining upon treatment with *Pe* in the anterior (B') and posterior midgut (B''). Quantifications of Dh31 signal intensity levels and cell numbers in the anterior (C') and posterior midgut (C''). (D) DNA mRNA expression value in the anterior and posterior midgut in sucrose and *Pe* treated animals. (E) Ex-vivo visualization of GCamp7c expression in Dh31+ cells in the anterior midgut of flies treated with 5% sucrose or *Pe* for 0h, 4h, 8h and 16h. (F) Quantification of (E). (G) Ex-

vivo visualization of GCamp7c expression in Dh31+ cells in the posterior midgut of flies not treated or treated with 5% sucrose or *Pe* for 16h. Dashed delineate the edges of the midgut. (C', C'', D) Two-tailed unpaired Student's t-test and Two-way ANOVA followed by Tukey's multiple comparisons test**.** * (P<0.1) ** (P<0.002) **** (P<0.0001).

**Figure 3: Gut epithelial derived reactive oxygen species induce Dh31 production in *Drosophila*** (A) Expression levels of Dh31 detected by immunostaining upon treatment with sucrose, *Pe* or *Pe* + NAC in the anterior midgut. (B) Quantifications of Dh31 signal intensity value and cell numbers in the anterior midguts from A. (C) Duox knockdown in ECs (*MexG4*) and effect on Dh31 protein levels in flies treated with sucrose and Pe (anterior midgut). (D) Quantifications of Dh31 signal intensity value and cell numbers in the anterior midguts from C. (E) Expression levels of Dh31 upon treatment with sucrose or hydrogen peroxide ($H_2O_2$). Quantifications of Dh31 signal intensity value and cell numbers in the anterior midguts from (E). Dashed delineate the edges of the midgut. (B) Ordinary one-way ANOVA and (D) Two-way ANOVA followed by Tukey's multiple comparisons test. (F) Two-tailed unpaired Student's t-test. * (P<0.04), ** (P<0.008), *** (P<0.003), **** (P<0.0001).

**Figure 4**: **Tracheal Dh31 receptor signaling is required for ISC proliferation during midgut regeneration. (A)** Expression pattern of *Dh31R* knock-in *Gal4* visualized by GFP in the whole midgut. (B) Additional anterior and posterior midgut regions highlighting Dh31R>GFP expression in TTCs. (C) Quantification of PH3+ cells in the posterior midgut of animals treated with sucrose or *Pe* following *Dh31R* knockdown (*Dh31R*-IR1, *Dh31R*-IR2 and *Dh31R*-IR3) in TTCS. (D) Quantification of PH3+ cells in the anterior and posterior midgut of animals treated with sucrose or *Pe* following Dh31R knockdown (*Dh31R*-IR1). (E) Quantification of PH3+ cells in the posterior midgut of animals treated with sucrose or Bleomycin following *Dh31R* knockdown (*Dh31R*-IR1). (C, D, E) Two-way ANOVA followed by Tukey's multiple comparisons test. ** (P<0.009), *** (P<0.002), **** (P<0.0001).

**Figure 5**: Tracheal coverage (A) and quantification (B) on posterior midguts of *Dh31R* knockdown (*Dh31R*-IR1 and *Dh31R*-IR2) in TTCs in animals treated with sucrose or *Pe*. Dashed delineate the edges of the midgut. (C) Representative confocal images of pERK (MAPK) immunostaining in the posterior midgut upon *Dh31R* KD (*Dh31R*-IR1) in TTCs of flies treated with sucrose or Pe. pERK is indicated in a fire scale (blue = low, yellow = high) to facilitate signal intensity visualization. Arrows indicate pERK signal in ISCs/EBs (small nuclei stained with anti-Armadillo (Arm) (white). (D) Quantification of pERK signal intensity in ISC/EB, as in C. Quantification of PH3+ cells (E) and Tracheal coverage (F) in the posterior midgut of animals treated with sucrose or Pe following *Pvf1* knockdown (*Pvf1*-IR1 and *Pvf1*-IR2) in TTCs. (G) Representative images of F. (H) Quantification of PH3+ cells in the posterior midgut of animals treated with sucrose or Pe following *Pvf1* knockdown (*Pvf1*-IR1) in ISCs/EBs. (I) Representative confocal images of pERK immunostaining in the posterior midgut upon Pvr KD (Pvr-IR1) in ISCs/EBs after treatment with sucrose or *Pe.* ISC/EBs (GFP, green) pERK (red). Dashed lines represent a magnified view of cells. (J) Quantification of pERK signal in ISC/EBs from I. (B, D, E, F, H, J) Two-way ANOVA followed by Tukey's multiple comparisons test. * (P<0.1), **** (P<0.0001).

**Figure 6**: (A) Representative images of Pvf1-HA (red) reporter co-localization with GFP driven by Dh31R-G4 in the anterior and posterior midgut of animals fed *Pe*. Arrows indicate Pvf1 co-localization with TTCs. (B) Pvf1 immunostaining in posterior midguts upon *Dh31R* KD (*Dh31R*-IR1) in TTCs (green) in animals fed sucrose or *Pe*. Squares represent a magnified view of TTCs cells. Magnified cells are colored in white and in fire scale to facilitate visualization. (C) Relative Pvf1 signal intensity in TTCs as in B. (D) Representative confocal images of Pvf1 (in fire color scale) immunostaining in the posterior midgut upon Dh31-KD (*Dh31*-IR) in neurons driven by the pan-neuronal line *nSybG4.* (E) Quantification of Pvf1 signal intensity in TTCs as in D. (F) Representative confocal images of Pvf1 immunostaining in the posterior midgut of animals fed sucrose or *Pe* with or without NAC. TTCs (green/white), Pvf1 (red/white). Squares represent a magnified view of TTCs cells. Dashed delineate the edges of the midgut. (G) Quantification of Pvf1 signal intensity levels in TTCs as in D. (C, E, G) Two-way ANOVA followed by Tukey's multiple comparisons test. **** (P<0.0001).

**Supplementary Figure 1**: (A, B) Quantification of PH3+ cells in the posterior midgut of animals treated with sucrose or *Pe* following different peptide hormones knockdown in EEs with *voilaG4*. (C) Dh31 immunostaining in the ventral nerve cord (VNC) and anterior midgut upon *Dh31* KD (*Dh31-IR2*) with a gut specific line *voilaG4,ChATG80*. Nc82 (neuronal markers, magenta), Dh31 (green). (D) Representative images of Dh31 immunostaining upon overexpression of VR in Dh31+ cells and treatment with Capsaicin. (E) Quantification of PH3+ cells in control and overexpression of *VR* or *VR* and *Dh31* in Dh31+ cells in animals treated with sucrose or Capsaicin. (F) Confocal images of nSyb>GFP expression pattern in the *Drosophila* hindgut and posterior midgut and co-localization with immunostainings for PDF (white) and Dh31 (red). Dashed square lines represent a magnified view. (G) RT-qPCR of *Dh31* mRNA levels upon *Dh31* KD *(Dh31*-IR2) with the neuronal driver nSybGal4. (H) Quantification of PH3+ cells in sucrose and *Pe* treated anterior and posterior midguts following *Dh31* knockdown (*Dh31*-IR1) with *nSybG4*. Gray dots represent individual cells and red dots represent the average value per midgut. (A, B, E, H) Two-way ANOVA followed by Tukey's multiple comparisons test. (G) Two-tailed unpaired Student's t-test. * (P<0,04), ** (P<0,008), *** (P<0.001), **** (P<0.0001).

**Supplementary Figure 2**: (A) Dh31 expression pattern in the midgut labeled with anti-Dh31 or GFP driven by Dh31G4. (B) Co-localization of GCamp7 (cytoplasmic green) and RedStinger (nuclear red) driven by Dh31 knock in Gal4 in animals fed sucrose or *Pe* for 16h. Dashed delineate the edges of the midgut.

**Supplementary Figure 3**: (A) Expression levels of Dh31 in the posterior midgut upon treatment with sucrose or hydrogen peroxide ($H_2O_2$). (B) Quantifications of Dh31 signal intensity value and cell numbers in the anterior midguts from A. Dashed delineate the edges of the midgut. Gray dots represent individual cells and red dots represent the average value per midgut. (B) Two-tailed unpaired Student's t-test. ** (P<0.006).

**Supplementary Figure 4:** (A) Expression pattern of Dh31R knock-in Gal4 visualized by GFP in enteric neurons, visceral muscle and enterocytes. (B) Co-localization of GFP in enteric neurons, as in A, with anti-PDF. (C) Quantification of PH3+ cells in the posterior midgut of animals treated with sucrose or *Pe* following *Dh31R* knockdown (*Dh31R*-IR1) in enteric neurons (C), visceral muscel (D) and enterocytes (E). (F). Quantification of PH3+ cells in the posterior midgut of animals treated with sucrose or *Pe* following *Dh31R* knockdown with 2 RNAis (*Dh31R*-IR1, *Dh31R*-IR1) in TTCs. (C, D, E, F) Two-way ANOVA followed by Tukey's multiple comparisons test. * (P<0,03), ** (P<0,009), **** (P<0.0001).

**Supplementary Figure 5**: (A) Representative confocal images of bnl-LacZ reporter immunostaining in the posterior midgut upon *Dh31R* KD (*Dh31R*-IR1) in TTCs after treatment with sucrose or *Pe.* Arrows indicate TTCs. TTCs (GFP, green) bln-LacZ (B-Gal, red/white). (B) Quantification of bnl-LacZ signal intensity values in TTCs from A. Gray dots represent single cell values. Black or red dots represent average per midgut. (C) List of genes related to secreted molecules with significant binding of Polymerase II identified with a published TaDa dateset in TTCs. Tracheal coverage (D) and quantification (E) on posterior midguts of *Pvf1* knockdown (*Pvf1*-IR1 and *Pvf1*-IR2) in TTCs in animals treated with sucrose or *Pe*. TTCs (green). (F) Quantification of PH3+ cells in the posterior midgut of animals treated with sucrose or *Pe* from E. (B, E, F) Two-way ANOVA followed by Tukey's multiple comparisons test. ** (P<0.003), **** (P<0.0001).

**Supplementary Figure 6**: (A) Pvf1-HA reporter levels in the anterior and posterior midguts treated with sucrose or *Pe.* TTCs (green), Pvf1 (red/white). Squares represent a magnified view of TTCs cells. (B) Working model.

## References


AMCHESLAVSKY, A., JIANG, J. & IP, Y. T. 2009. Tissue damage-induced intestinal stem cell division in Drosophila. *Cell Stem Cell,* 4**,** 49-61.

AMCHESLAVSKY, A., SONG, W., LI, Q., NIE, Y., BRAGATTO, I., FERRANDON, D., PERRIMON, N. & IP, Y. T. 2014. Enteroendocrine cells support intestinal stem-cell-mediated homeostasis in Drosophila. *Cell Rep,* 9**,** 32-39.

BALDASSANO, S. & AMATO, A. 2014. GLP-2: What do we know? What are we going to discover? *Regulatory Peptides,* 194-195**,** 6-10.

BENGUETTAT, O., JNEID, R., SOLTYS, J., LOUDHAIEF, R., BRUN-BARALE, A., OSMAN, D. & GALLET, A. 2018. The DH31/CGRP enteroendocrine peptide triggers intestinal contractions favoring the elimination of opportunistic bacteria. *PLOS Pathogens,* 14**,** e1007279.

BEUMER, J., PUSCHHOF, J., BAUZÁ-MARTINEZ, J., MARTÍNEZ-SILGADO, A., ELMENTAITE, R., JAMES, K. R., ROSS, A., HENDRIKS, D., ARTEGIANI, B., BUSSLINGER, G. A., PONSIOEN, B., ANDERSSON-ROLF, A., SAFTIEN, A., BOOT, C., KRETZSCHMAR, K., GEURTS, M. H., BAR-EPHRAIM, Y. E., PLEGUEZUELOS-MANZANO, C., POST, Y., BEGTHEL, H., VAN DER LINDEN, F., LOPEZ-IGLESIAS, C., VAN DE WETERING, W. J., VAN DER LINDEN, R., PETERS, P. J., HECK, A. J. R., GOEDHART, J., SNIPPERT, H., ZILBAUER, M., TEICHMANN, S. A., WU, W. & CLEVERS, H. 2020. High-Resolution mRNA and Secretome Atlas of Human Enteroendocrine Cells. *Cell,* 181**,** 1291-1306.e19.

BOND, D. & FOLEY, E. 2012. Autocrine platelet-derived growth factor-vascular endothelial growth factor receptor-related (Pvr) pathway activity controls intestinal stem cell proliferation in the adult Drosophila midgut. *J Biol Chem,* 287**,** 27359-70.

BOSI, G., SHINN, A. P., GIARI, L., SIMONI, E., PIRONI, F. & DEZFULI, B. S. 2005. Changes in the neuromodulators of the diffuse endocrine system of the alimentary canal of farmed rainbow trout, Oncorhynchus mykiss (Walbaum), naturally infected with Eubothrium crassum (Cestoda). *J Fish Dis,* 28**,** 703-11.

BUCHON, N., OSMAN, D., DAVID, F. P., FANG, H. Y., BOQUETE, J. P., DEPLANCKE, B. & LEMAITRE, B. 2013. Morphological and molecular characterization of adult midgut compartmentalization in Drosophila. *Cell Rep,* 3**,** 1725-38.

CHEN, J., XU, N., WANG, C., HUANG, P., HUANG, H., JIN, Z., YU, Z., CAI, T., JIAO, R. & XI, R. 2018. Transient Scute activation via a self-stimulatory loop directs enteroendocrine cell pair specification from self-renewing intestinal stem cells. *Nat Cell Biol,* 20**,** 152-161.

COGNIGNI, P., BAILEY, A. P. & MIGUEL-ALIAGA, I. 2011. Enteric Neurons and Systemic Signals Couple Nutritional and Reproductive Status with Intestinal Homeostasis. *Cell Metabolism,* 13**,** 92-104.

DAHLY, E. M., GILLINGHAM, M. B., GUO, Z., MURALI, S. G., NELSON, D. W., HOLST, J. J. & NEY, D. M. 2003. Role of luminal nutrients and endogenous GLP-2 in intestinal adaptation to mid-small bowel resection. *Am J Physiol Gastrointest Liver Physiol,* 284**,** G670-82.

DENG, B., LI, Q., LIU, X., CAO, Y., LI, B., QIAN, Y., XU, R., MAO, R., ZHOU, E., ZHANG, W., HUANG, J. & RAO, Y. 2019. Chemoconnectomics: Mapping Chemical Transmission in Drosophila. *Neuron,* 101**,** 876-893.e4.

DRUCKER, D. J., ERLICH, P., ASA, S. L. & BRUBAKER, P. L. 1996. Induction of intestinal epithelial proliferation by glucagon-like peptide 2. *Proc Natl Acad Sci U S A,* 93**,** 7911-6.

DUTTA, D., DOBSON, ADAM J., HOUTZ, PHILIP L., GLÄSSE, C., REVAH, J., KORZELIUS, J., PATEL, P. H., EDGAR, BRUCE A. & BUCHON, N. 2015. Regional Cell-Specific Transcriptome Mapping Reveals Regulatory Complexity in the Adult Drosophila Midgut. *Cell Reports,* 12**,** 346-358.

ESTALL, J. L. & DRUCKER, D. J. 2006. Glucagon-like Peptide-2. *Annu Rev Nutr,* 26**,** 391-411.

FORBES, A. B., WARREN, M., UPJOHN, M., JACKSON, B., JONES, J., CHARLIER, J. & FOX, M. T. 2009. Associations between blood gastrin, ghrelin, leptin, pepsinogen and Ostertagia ostertagi antibody concentrations and voluntary feed intake in calves exposed to a trickle infection with O. ostertagi. *Vet Parasitol,* 162**,** 295-305.

FURUYA, K., MILCHAK, R. J., SCHEGG, K. M., ZHANG, J., TOBE, S. S., COAST, G. M. & SCHOOLEY, D. A. 2000. Cockroach diuretic hormones: Characterization of a calcitonin-like peptide in insects. *Proceedings of the National Academy of Sciences,* 97**,** 6469-6474.

GEHART, H., VAN ES, J. H., HAMER, K., BEUMER, J., KRETZSCHMAR, K., DEKKERS, J. F., RIOS, A. & CLEVERS, H. 2019. Identification of Enteroendocrine Regulators by Real-Time Single-Cell Differentiation Mapping. *Cell,* 176**,** 1158-1173.e16.

GRIBBLE, F. M. & REIMANN, F. 2016. Enteroendocrine Cells: Chemosensors in the Intestinal Epithelium. *Annual Review of Physiology,* 78**,** 277-299.

GUO, X., LV, J. & XI, R. 2022. The specification and function of enteroendocrine cells in Drosophila and mammals: a comparative review. *Febs j,* 289**,** 4773-4796.

GUO, X., YIN, C., YANG, F., ZHANG, Y., HUANG, H., WANG, J., DENG, B., CAI, T., RAO, Y. & XI, R. 2019. The Cellular Diversity and Transcription Factor Code of Drosophila Enteroendocrine Cells. *Cell Reports,* 29**,** 4172-4185.e5.

HAGEMAN, J. H., HEINZ, M. C., KRETZSCHMAR, K., VAN DER VAART, J., CLEVERS, H. & SNIPPERT, H. J. G. 2020. Intestinal Regeneration: Regulation by the Microenvironment. *Developmental Cell,* 54**,** 435-446.

HARNACK, C., BERGER, H., ANTANAVICIUTE, A., VIDAL, R., SAUER, S., SIMMONS, A., MEYER, T. F. & SIGAL, M. 2019. R-spondin 3 promotes stem cell recovery and epithelial regeneration in the colon. *Nat Commun,* 10**,** 4368.

HARRISON, E., LAL, S. & MCLAUGHLIN, J. T. 2013. Enteroendocrine cells in gastrointestinal pathophysiology. *Curr Opin Pharmacol,* 13**,** 941-5.

HE, L., SI, G., HUANG, J., SAMUEL, A. D. T. & PERRIMON, N. 2018. Mechanical regulation of stem-cell differentiation by the stretch-activated Piezo channel. *Nature,* 555**,** 103-106.

HUNG, R. J., HU, Y., KIRCHNER, R., LIU, Y., XU, C., COMJEAN, A., TATTIKOTA, S. G., LI, F., SONG, W., HO SUI, S. & PERRIMON, N. 2020. A cell atlas of the adult Drosophila midgut. *Proc Natl Acad Sci U S A,* 117**,** 1514-1523.

JIANG, H., GRENLEY, M. O., BRAVO, M.-J., BLUMHAGEN, R. Z. & EDGAR, B. A. 2011. EGFR/Ras/MAPK Signaling Mediates Adult Midgut Epithelial Homeostasis and Regeneration in Drosophila. *Cell Stem Cell,* 8**,** 84-95.

JIANG, H., PATEL, P. H., KOHLMAIER, A., GRENLEY, M. O., MCEWEN, D. G. & EDGAR, B. A. 2009a. Cytokine/Jak/Stat Signaling Mediates Regeneration and Homeostasis in the Drosophila Midgut. *Cell,* 137**,** 1343-1355.

JIANG, H., PATEL, P. H., KOHLMAIER, A., GRENLEY, M. O., MCEWEN, D. G. & EDGAR, B. A. 2009b. Cytokine/Jak/Stat signaling mediates regeneration and homeostasis in the Drosophila midgut. *Cell,* 137**,** 1343-55.

KAMAREDDINE, L., ROBINS, W. P., BERKEY, C. D., MEKALANOS, J. J. & WATNICK, P. I. 2018. The Drosophila Immune Deficiency Pathway Modulates Enteroendocrine Function and Host Metabolism. *Cell Metab,* 28**,** 449-462.e5.

KIM, J.-E., FEI, L., YIN, W.-C., COQUENLORGE, S., RAO-BHATIA, A., ZHANG, X., SHI, S. S. W., LEE, J. H., HAHN, N. A., RIZVI, W., KIM, K.-H., SUNG, H.-K., HUI, C.-C., GUO, G. & KIM, T.-H. 2020. Single cell and genetic analyses reveal conserved populations and signaling mechanisms of gastrointestinal stromal niches. *Nature Communications,* 11**,** 334.

KITAMOTO, T. 2002. Conditional disruption of synaptic transmission induces male-male courtship behavior in Drosophila. *Proc Natl Acad Sci U S A,* 99**,** 13232-7.

KUROGI, Y., IMURA, E., MIZUNO, Y., HOSHINO, R., NOUZOVA, M., MATSUYAMA, S., MIZOGUCHI, A., KONDO, S., TANIMOTO, H., NORIEGA, F. G. & NIWA, R. 2023. Female reproductive dormancy in Drosophila is regulated by DH31-producing neurons projecting into the corpus allatum. *Development,* 150.

LEBRUN, L. J., LENAERTS, K., KIERS, D., PAIS DE BARROS, J. P., LE GUERN, N., PLESNIK, J., THOMAS, C., BOURGEOIS, T., DEJONG, C. H. C., KOX, M., HUNDSCHEID, I. H. R., KHAN, N. A., MANDARD, S., DECKERT, V., PICKKERS, P., DRUCKER, D. J., LAGROST, L. & GROBER, J. 2017. Enteroendocrine L Cells Sense LPS after Gut Barrier Injury to Enhance GLP-1 Secretion. *Cell Rep,* 21**,** 1160-1168.

LI, H., JANSSENS, J., DE WAEGENEER, M., KOLLURU, S. S., DAVIE, K., GARDEUX, V., SAELENS, W., DAVID, F. P. A., BRBIĆ, M., SPANIER, K., LESKOVEC, J., MCLAUGHLIN, C. N., XIE, Q., JONES, R. C., BRUECKNER, K., SHIM, J., TATTIKOTA, S. G., SCHNORRER, F., RUST, K., NYSTUL, T. G., CARVALHO-SANTOS, Z., RIBEIRO, C., PAL, S., MAHADEVARAJU, S., PRZYTYCKA, T. M., ALLEN, A. M., GOODWIN, S. F., BERRY, C. W., FULLER, M. T., WHITE-COOPER, H., MATUNIS, E. L., DINARDO, S., GALENZA, A., O'BRIEN, L. E., DOW, J. A. T., JASPER, H., OLIVER, B., PERRIMON, N., DEPLANCKE, B., QUAKE, S. R., LUO, L., AERTS, S., AGARWAL, D., AHMED-BRAIMAH, Y., ARBEITMAN, M., ARISS, M. M., AUGSBURGER, J., AYUSH, K., BAKER, C. C., BANISCH, T., BIRKER, K., BODMER, R., BOLIVAL, B., BRANTLEY, S. E., BRILL, J. A., BROWN, N. C., BUEHNER, N. A., CAI, X. T., CARDOSO-FIGUEIREDO, R., CASARES, F., CHANG, A., CLANDININ, T. R., CRASTA, S., DESPLAN, C., DETWEILER, A. M., DHAKAN, D. B., DONÀ, E., ENGERT, S., FLOC'HLAY, S., GEORGE, N., GONZÁLEZ-SEGARRA, A. J., GROVES, A. K., GUMBIN, S., GUO, Y., HARRIS, D. E., HEIFETZ, Y., HOLTZ, S. L., HORNS, F., HUDRY, B., HUNG, R.-J., JAN, Y. N., JASZCZAK, J. S., JEFFERIS, G. S. X. E., KARKANIAS, J., KARR, T. L., KATHEDER, N. S., KEZOS, J., KIM, A. A., KIM, S. K., KOCKEL, L., KONSTANTINIDES, N., KORNBERG, T. B., KRAUSE, H. M., LABOTT, A. T., LATURNEY, M., LEHMANN, R., LEINWAND, S., LI, J., LI, J. S. S., LI, K., et al. 2022. Fly Cell Atlas: A single-nucleus transcriptomic atlas of the adult fruit fly. *Science,* 375**,** eabk2432.

LIN, H. H., KUANG, M. C., HOSSAIN, I., XUAN, Y., BEEBE, L., SHEPHERD, A. K., ROLANDI, M. & WANG, J. W. 2022. A nutrient-specific gut hormone arbitrates between courtship and feeding. *Nature,* 602**,** 632-638.

LIU, X., NAGY, P., BONFINI, A., HOUTZ, P., BING, X. L., YANG, X. & BUCHON, N. 2022a. Microbes affect gut epithelial cell composition through immune-dependent regulation of intestinal stem cell differentiation. *Cell Rep,* 38**,** 110572.

LIU, Y., LI, J. S. S., RODIGER, J., COMJEAN, A., ATTRILL, H., ANTONAZZO, G., BROWN, N. H., HU, Y. & PERRIMON, N. 2022b. FlyPhoneDB: an integrated web-based resource for cell-cell communication prediction in Drosophila. *Genetics,* 220.

MANION, J., MUSSER, M. A., KUZIEL, G. A., LIU, M., SHEPHERD, A., WANG, S., LEE, P.-G., ZHAO, L., ZHANG, J., MARREDDY, R. K. R., GOLDSMITH, J. D., YUAN, K., HURDLE, J. G., GERHARD, R., JIN, R., RAKOFF-NAHOUM, S., RAO, M. & DONG, M. 2023. C. difficile intoxicates neurons and pericytes to drive neurogenic inflammation. *Nature,* 622**,** 611-618.

MARTIN, G. R., WALLACE, L. E., HARTMANN, B., HOLST, J. J., DEMCHYSHYN, L., TONEY, K. & SIGALET, D. L. 2005. Nutrient-stimulated GLP-2 release and crypt cell proliferation in experimental short bowel syndrome. *Am J Physiol Gastrointest Liver Physiol,* 288**,** G431-8.

MCCARTHY, N., MANIERI, E., STORM, E. E., SAADATPOUR, A., LUOMA, A. M., KAPOOR, V. N., MADHA, S., GAYNOR, L. T., COX, C., KEERTHIVASAN, S., WUCHERPFENNIG, K., YUAN, G. C., DE SAUVAGE, F. J., TURLEY, S. J. & SHIVDASANI, R. A. 2020. Distinct Mesenchymal Cell Populations Generate the Essential Intestinal BMP Signaling Gradient. *Cell Stem Cell,* 26**,** 391-402.e5.

MEDINA, A., BELLEC, K., POLCOWÑUK, S. & CORDERO, J. B. 2022. Investigating local and systemic intestinal signalling in health and disease with Drosophila. *Dis Model Mech,* 15.

MISHIMA, T., ITO, Y., HOSONO, K., TAMURA, Y., UCHIDA, Y., HIRATA, M., SUZSUKI, T., AMANO, H., KATO, S., KURIHARA, Y., KURIHARA, H., HAYASHI, I., WATANABE, M. & MAJIMA, M. 2011. Calcitonin gene-related peptide facilitates revascularization during hindlimb ischemia in mice. *Am J Physiol Heart Circ Physiol,* 300**,** H431-9.

MORRIS, O. & JASPER, H. 2021. Reactive Oxygen Species in intestinal stem cell metabolism, fate and function. *Free Radic Biol Med,* 166**,** 140-146.

NIEC, R. E., CHU, T., SCHERNTHANNER, M., GUR-COHEN, S., HIDALGO, L., PASOLLI, H. A., LUCKETT, K. A., WANG, Z., BHALLA, S. R., CAMBULI, F., KATARU, R. P., GANESH, K., MEHRARA, B. J., PE'ER, D. & FUCHS, E. 2022. Lymphatics act as a signaling hub to regulate intestinal stem cell activity. *Cell Stem Cell,* 29**,** 1067-1082.e18.

OVINGTON, K. S. 1985. Dose-dependent relationships between Nippostrongylus brasiliensis populations and rat food intake. *Parasitology,* 91 ( Pt 1)**,** 157-67.

PARIKH, K., ANTANAVICIUTE, A., FAWKNER-CORBETT, D., JAGIELOWICZ, M., AULICINO, A., LAGERHOLM, C., DAVIS, S., KINCHEN, J., CHEN, H. H., ALHAM, N. K., ASHLEY, N., JOHNSON, E., HUBLITZ, P., BAO, L., LUKOMSKA, J., ANDEV, R. S., BJÖRKLUND, E., KESSLER, B. M., FISCHER, R., GOLDIN, R., KOOHY, H. & SIMMONS, A. 2019. Colonic epithelial cell diversity in health and inflammatory bowel disease. *Nature,* 567**,** 49-55.

PARSONS, B. & FOLEY, E. 2013. The Drosophila platelet-derived growth factor and vascular endothelial growth factor-receptor related (Pvr) protein ligands Pvf2 and Pvf3 control hemocyte viability and invasive migration. *J Biol Chem,* 288**,** 20173-83.

PEROCHON, J., YU, Y., AUGHEY, G. N., MEDINA, A. B., SOUTHALL, T. D. & CORDERO, J. B. 2021. Dynamic adult tracheal plasticity drives stem cell adaptation to changes in intestinal homeostasis in Drosophila. *Nat Cell Biol,* 23**,** 485-496.

PETSAKOU, A., LIU, Y., LIU, Y., COMJEAN, A., HU, Y. & PERRIMON, N. 2023. Epithelial Ca(2+) waves triggered by enteric neurons heal the gut. *bioRxiv*.

RUSSELL, F. A., KING, R., SMILLIE, S. J., KODJI, X. & BRAIN, S. D. 2014. Calcitonin gene-related peptide: physiology and pathophysiology. *Physiol Rev,* 94**,** 1099-142.

SASAKI, M., FITZGERALD, A. J., MANDIR, N., SASAKI, K., WRIGHT, N. A. & GOODLAD, R. A. 2001. Glicentin, an active enteroglucagon, has a significant trophic role on the small intestine but not on the colon in the rat. *Aliment Pharmacol Ther,* 15**,** 1681-6.

SCIOLA, V., MASSIRONI, S., CONTE, D., CAPRIOLI, F., FERRERO, S., CIAFARDINI, C., PERACCHI, M., BARDELLA, M. T. & PIODI, L. 2009. Plasma chromogranin a in patients with inflammatory bowel disease. *Inflamm Bowel Dis,* 15**,** 867-71.

SCOPELLITI, A., BAUER, C., YU, Y., ZHANG, T., KRUSPIG, B., MURPHY, D. J., VIDAL, M., MADDOCKS, O. D. K. & CORDERO, J. B. 2018. A Neuronal Relay Mediates a Nutrient Responsive Gut/Fat Body Axis Regulating Energy Homeostasis in Adult Drosophila. *Cell Metab*.

SCOPELLITI, A., CORDERO, J. B., DIAO, F., STRATHDEE, K., WHITE, B. H., SANSOM, O. J. & VIDAL, M. 2014. Local control of intestinal stem cell homeostasis by enteroendocrine cells in the adult Drosophila midgut. *Curr Biol,* 24**,** 1199-211.

STZEPOURGINSKI, I., NIGRO, G., JACOB, J.-M., DULAUROY, S., SANSONETTI, P. J., EBERL, G. & PEDUTO, L. 2017. CD34<sup>+</sup> mesenchymal cells are a major component of the intestinal stem cells niche at homeostasis and after injury. *Proceedings of the National Academy of Sciences,* 114**,** E506-E513.

TAMAMOUNA, V., RAHMAN, M. M., PETERSSON, M., CHARALAMBOUS, I., KUX, K., MAINOR, H., BOLENDER, V., ISBILIR, B., EDGAR, B. A. & PITSOULI, C. 2021. Remodelling of oxygen-transporting tracheoles drives intestinal regeneration and tumorigenesis in Drosophila. *Nat Cell Biol,* 23**,** 497-510.

TAUC, H. M., RODRIGUEZ-FERNANDEZ, I. A., HACKNEY, J. A., PAWLAK, M., RONNEN ORON, T., KORZELIUS, J., MOUSSA, H. F., CHAUDHURI, S., MODRUSAN, Z., EDGAR, B. A. & JASPER, H.

2021. Age-related changes in polycomb gene regulation disrupt lineage fidelity in intestinal stem cells. *Elife,* 10.
TODA, M., SUZUKI, T., HOSONO, K., KURIHARA, Y., KURIHARA, H., HAYASHI, I., KITASATO, H., HOKA, S. & MAJIMA, M. 2008. Roles of calcitonin gene-related peptide in facilitation of wound healing and angiogenesis. *Biomed Pharmacother,* 62**,** 352-9.
VAN MARLE, G., SHARKEY, K. A., GILL, M. J. & CHURCH, D. L. 2013. Gastrointestinal viral load and enteroendocrine cell number are associated with altered survival in HIV-1 infected individuals. *PLoS One,* 8**,** e75967.
VEENSTRA, J. A., AGRICOLA, H. J. & SELLAMI, A. 2008. Regulatory peptides in fruit fly midgut. *Cell Tissue Res,* 334**,** 499-516.
WORTHINGTON, J. J., REIMANN, F. & GRIBBLE, F. M. 2018. Enteroendocrine cells-sensory sentinels of the intestinal environment and orchestrators of mucosal immunity. *Mucosal Immunol,* 11**,** 3-20.
XU, H., DING, J., PORTER, C. B. M., WALLRAPP, A., TABAKA, M., MA, S., FU, S., GUO, X., RIESENFELD, S. J., SU, C., DIONNE, D., NGUYEN, L. T., LEFKOVITH, A., ASHENBERG, O., BURKETT, P. R., SHI, H. N., ROZENBLATT-ROSEN, O., GRAHAM, D. B., KUCHROO, V. K., REGEV, A. & XAVIER, R. J. 2019. Transcriptional Atlas of Intestinal Immune Cells Reveals that Neuropeptide α-CGRP Modulates Group 2 Innate Lymphoid Cell Responses. *Immunity,* 51**,** 696-708.e9.
YANG, S., GAAFAR, S. M. & BOTTOMS, G. D. 1990. Effects of multiple dose infections with Ascaris suum on blood gastrointestinal hormone levels in pigs. *Vet Parasitol,* 37**,** 31-44.
ZHANG, X., ZHANG, H., SHEN, B. & SUN, X. F. 2019. Chromogranin-A Expression as a Novel Biomarker for Early Diagnosis of Colon Cancer Patients. *Int J Mol Sci,* 20.
ZHOU, J. & BOUTROS, M. 2023. Intestinal stem cells and their niches in homeostasis and disease. *Cells & Development,* 175**,** 203862.
ZISSIMOPOULOS, A., VRADELIS, S., KONIALIS, M., CHADOLIAS, D., BAMPALI, A., CONSTANTINIDIS, T., EFREMIDOU, E. & KOUKLAKIS, G. 2014. Chromogranin A as a biomarker of disease activity and biologic therapy in inflammatory bowel disease: a prospective observational study. *Scand J Gastroenterol,* 49**,** 942-9.

**Acknowledgements:** We would like to thank Irene Miguel-Aliaga, Henrike Scholz, Jan Veentra, Benny Shilo and Jing W.Wang for generously sharing flies and reagents. We thank the Bloomington Drosophila Stock Center; the Vienna Drosophila Resource Center and the *Drosophila* Studies Hybridoma Bank for fly stocks and antibodies. We would like to thank the Core Services and Advanced Technologies at the CRUK Scotland Institute, which is core funded by Cancer Research UK (A31287). With particular thanks to Leo Carlin, Claire Mitchell and Peter Thomason from the Beatson Advanced Imaging Resource, and Colin Nixon and the Histology Laboratory for assistance with mouse sample preparation and staining. We thank all members of the Cordero laboratory for general advice on the project.

**Funding sources:**

Work in the Cordero laboratory is funded through a Wellcome Trust and Royal Society Sir Henry Dale Fellowship (104103/Z/14/Z), and Wellcome Trust Senior Research Fellowship (223091/Z/21/Z) to J.B.C., core Institutional funds from CRUK to the CRUK Scotland Institute (A31287), a Wellcome ISSF Returner Scheme and Tenovus Fellowships to J.P, and a China Scholarship Council studentship to Y.T. (202006910022).

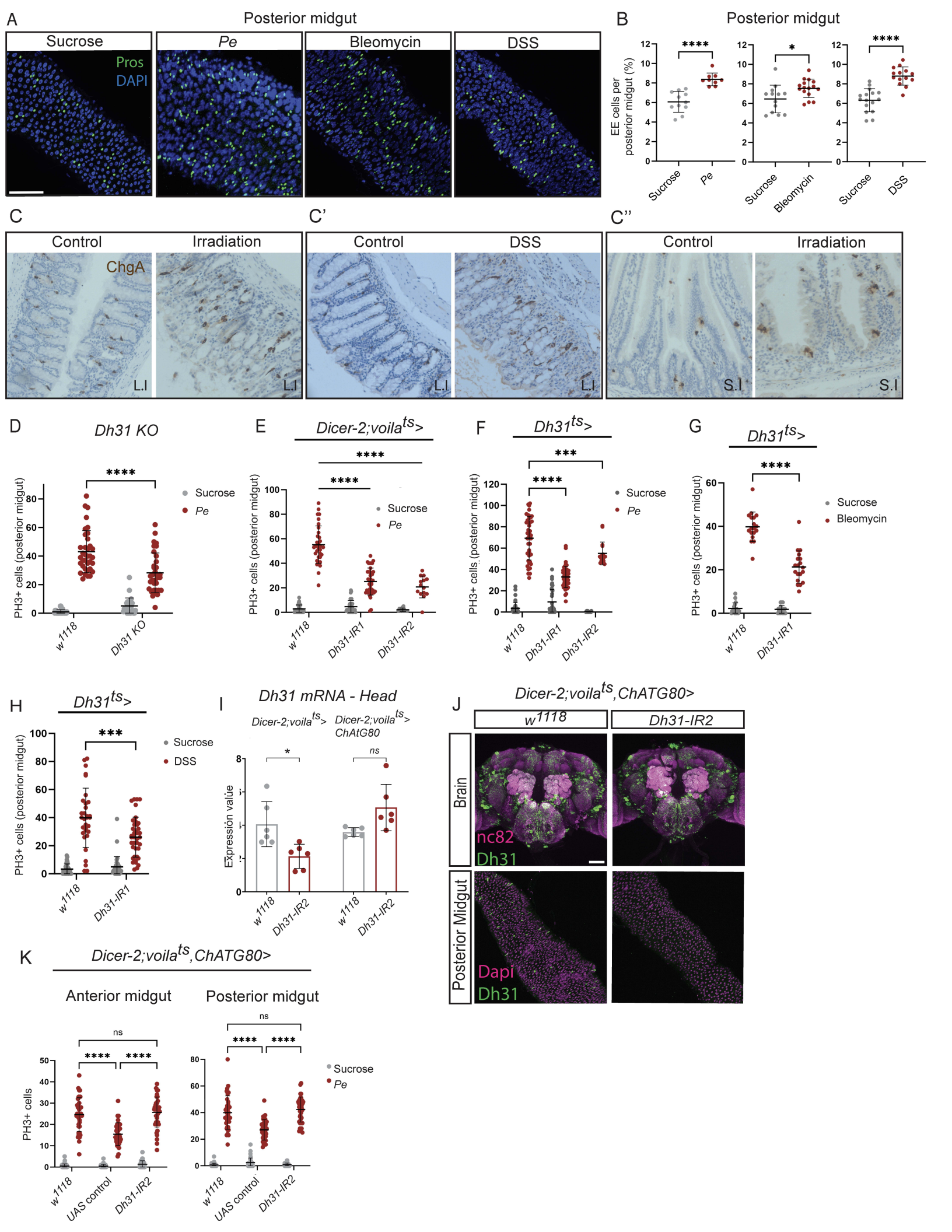
A
Posterior midgut
Sucrose
Pe
Bleomycin
DSS
Pros
DAPI
B
Posterior midgut
EE cells per posterior midgut (%)
Sucrose
Pe
Bleomycin
DSS
C
C'
C''
Control
Irradiation
DSS
ChgA
L.I
S.I
D
Dh31 KO
PH3+ cells (posterior midgut)
w1118
Dh31 KO
E
Dicer-2;voilaTS>
Dh31-IR1
Dh31-IR2
F
Dh31TS>
G
H
I
Dh31 mRNA - Head
Dicer-2;voilaTS>
Dicer-2;voilaTS> ChAtG80
Expression value
J
Dicer-2;voilaTS,ChATG80>
Brain
Posterior Midgut
nc82
Dh31
Dapi
K
Anterior midgut
Posterior midgut
UAS control
ns

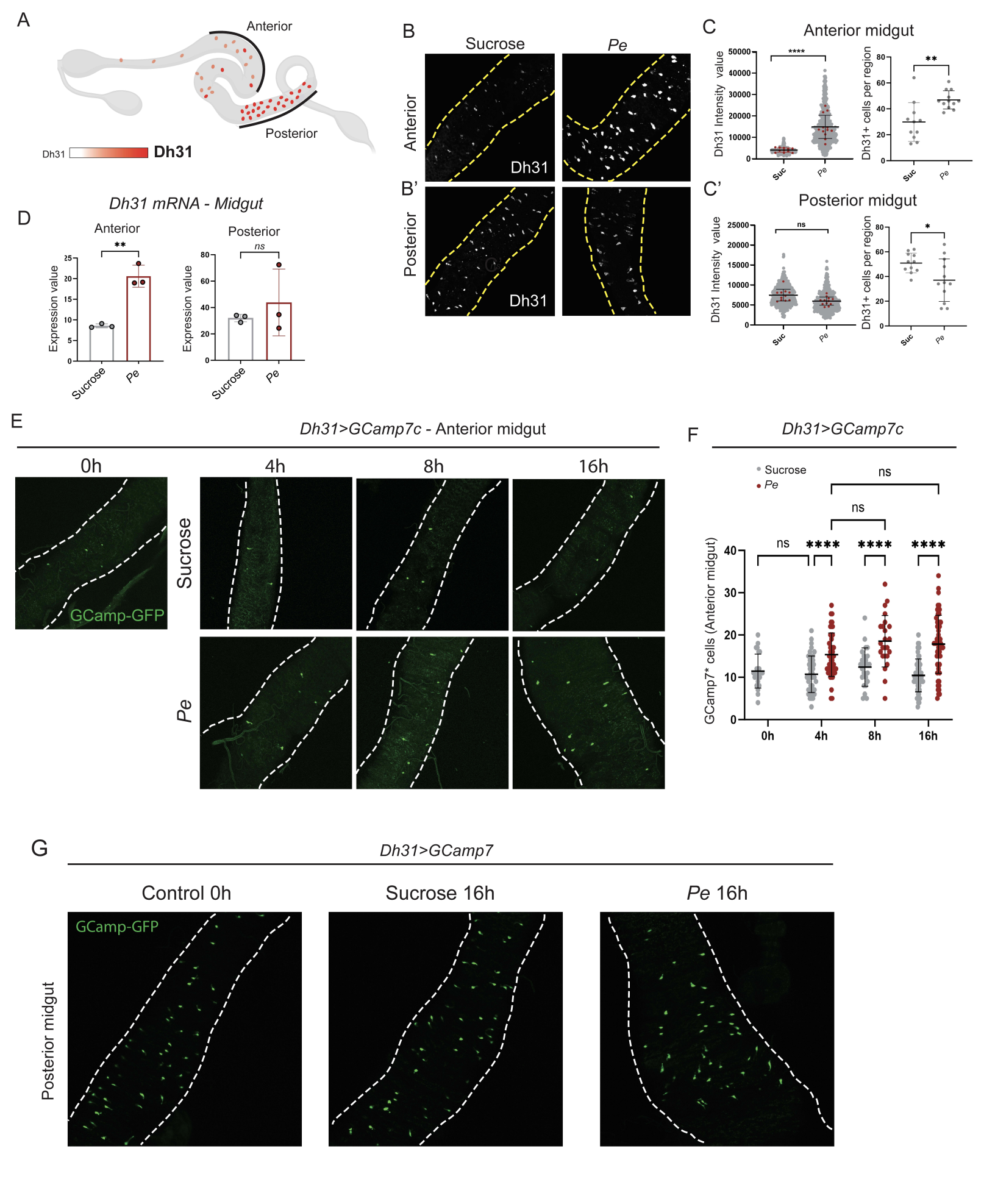
A
Anterior
Posterior
Dh31
Dh31
B
Sucrose
Pe
Anterior
Posterior
Dh31
Dh31
B'
C
Anterior midgut
Dh31 Intensity value
Dh31+ cells per region
Suc
Pe
C'
Posterior midgut
D
Dh31 mRNA - Midgut
Anterior
Posterior
Expression value
Sucrose
Pe
E
Dh31>GCamp7c - Anterior midgut
0h
4h
8h
16h
Sucrose
Pe
GCamp-GFP
F
Dh31>GCamp7c
Sucrose
Pe
GCamp7* cells (Anterior midgut)
ns
****
G
Dh31>GCamp7
Control 0h
Sucrose 16h
Pe 16h
Posterior midgut
GCamp-GFP

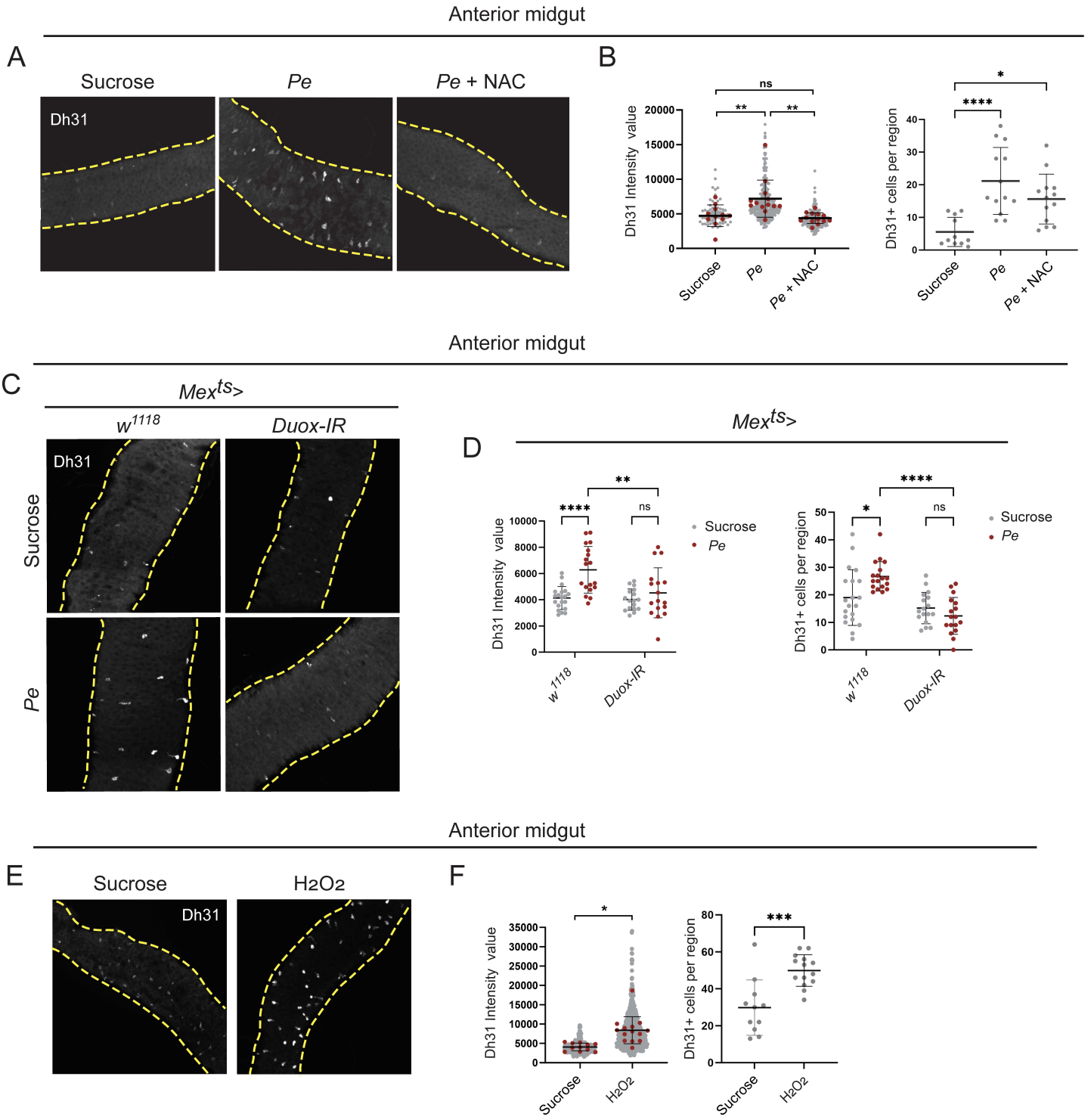
Anterior midgut
A
Sucrose
Pe
Pe + NAC
Dh31
B
Dh31 Intensity value
Dh31+ cells per region
ns
**
**
*
****
Sucrose
Pe
Pe + NAC
Anterior midgut
C
Mex^ts>
w^1118
Duox-IR
Sucrose
Pe
Dh31
D
Mex^ts>
Dh31 Intensity value
Dh31+ cells per region
****
**
ns
*
****
ns
Sucrose
Pe
w^1118
Duox-IR
Anterior midgut
E
Sucrose
H2O2
Dh31
F
Dh31 Intensity value
Dh31+ cells per region
*
***
Sucrose
H2O2

A

*Dh31R>mCD8-GFP*

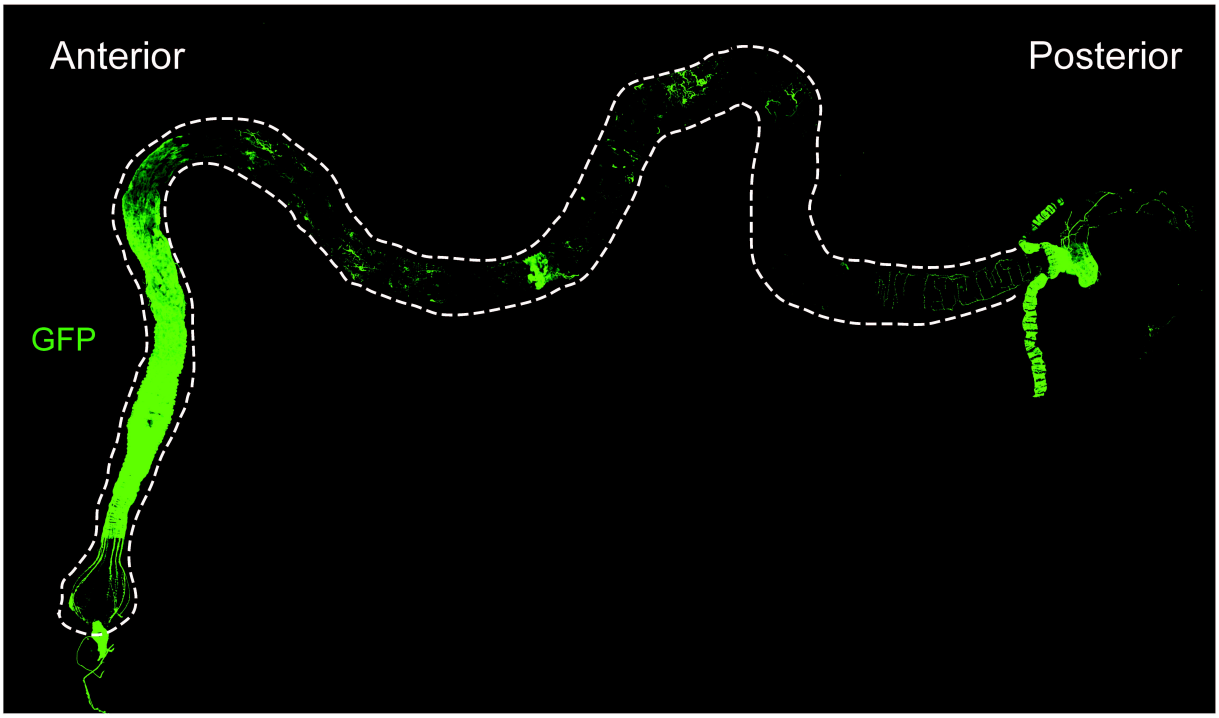


B

Terminal trachea cells

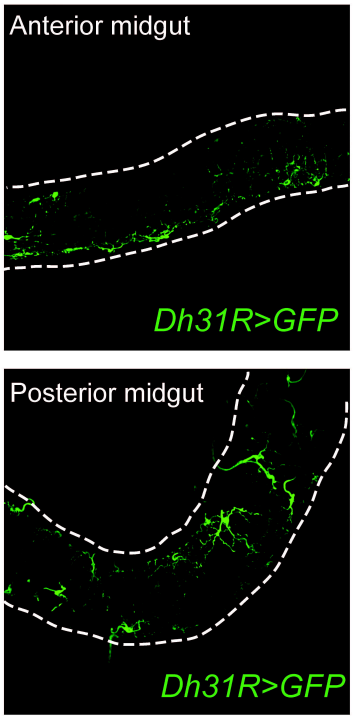


*dSRF*$^{ts}$>GFP

C

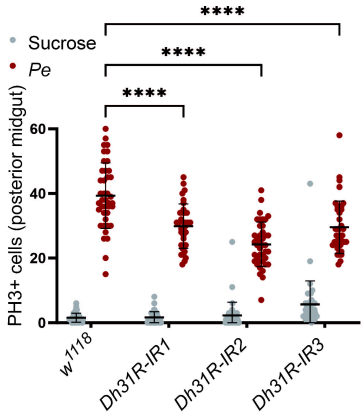


D

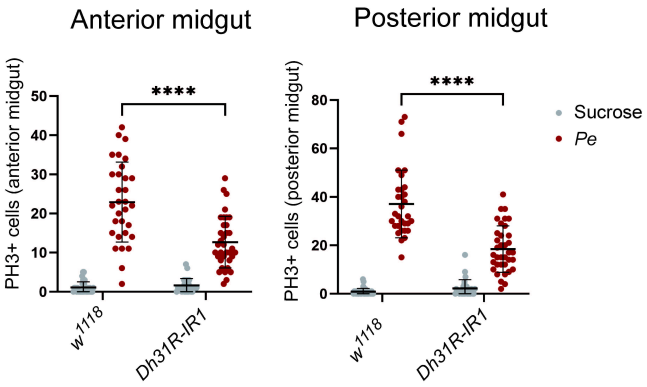


E

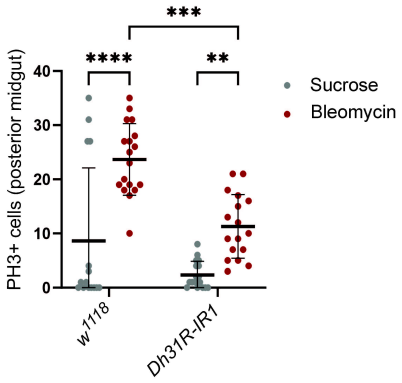

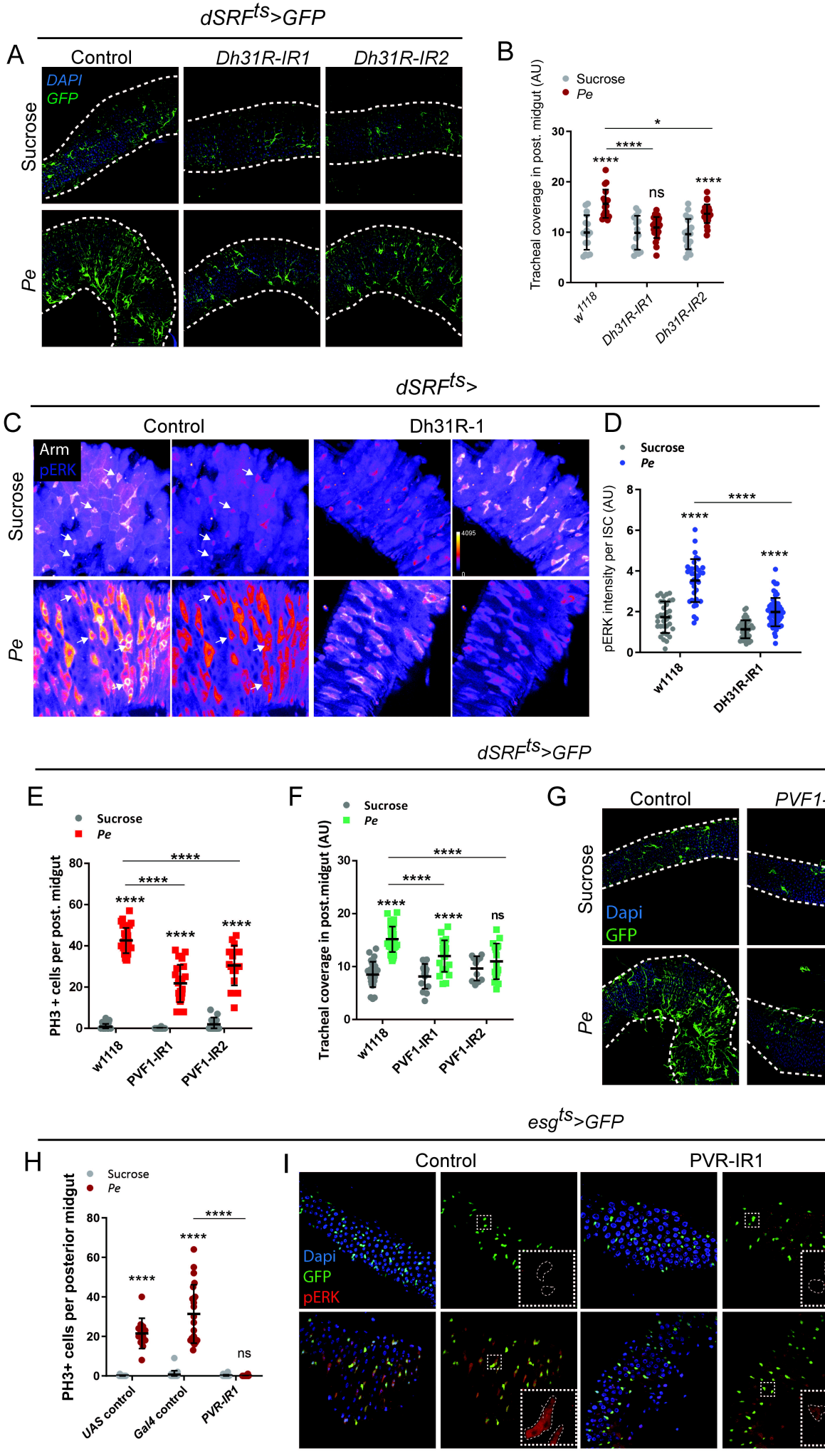
dSRF^ts>GFP
A
Control
Dh31R-IR1
Dh31R-IR2
DAPI
GFP
Sucrose
Pe
B
Sucrose
Pe
Tracheal coverage in post. midgut (AU)
w1118
Dh31R-IR1
Dh31R-IR2
dSRF^ts>
C
Control
Dh31R-1
Arm
pERK
D
pERK intensity per ISC (AU)
w1118
DH31R-IR1
dSRF^ts>GFP
E
PH3 + cells per post. midgut
w1118
PVF1-IR1
PVF1-IR2
F
Tracheal coverage in post.midgut (AU)
G
PVF1-IR1
PVF1-IR2
Dapi
esg^ts>GFP
H
PH3+ cells per posterior midgut
UAS control
Gal4 control
PVR-IR1
I
PVR-IR1
pERK
J
P-erk intensity relative to background per ISCs/EBs (a.u.)

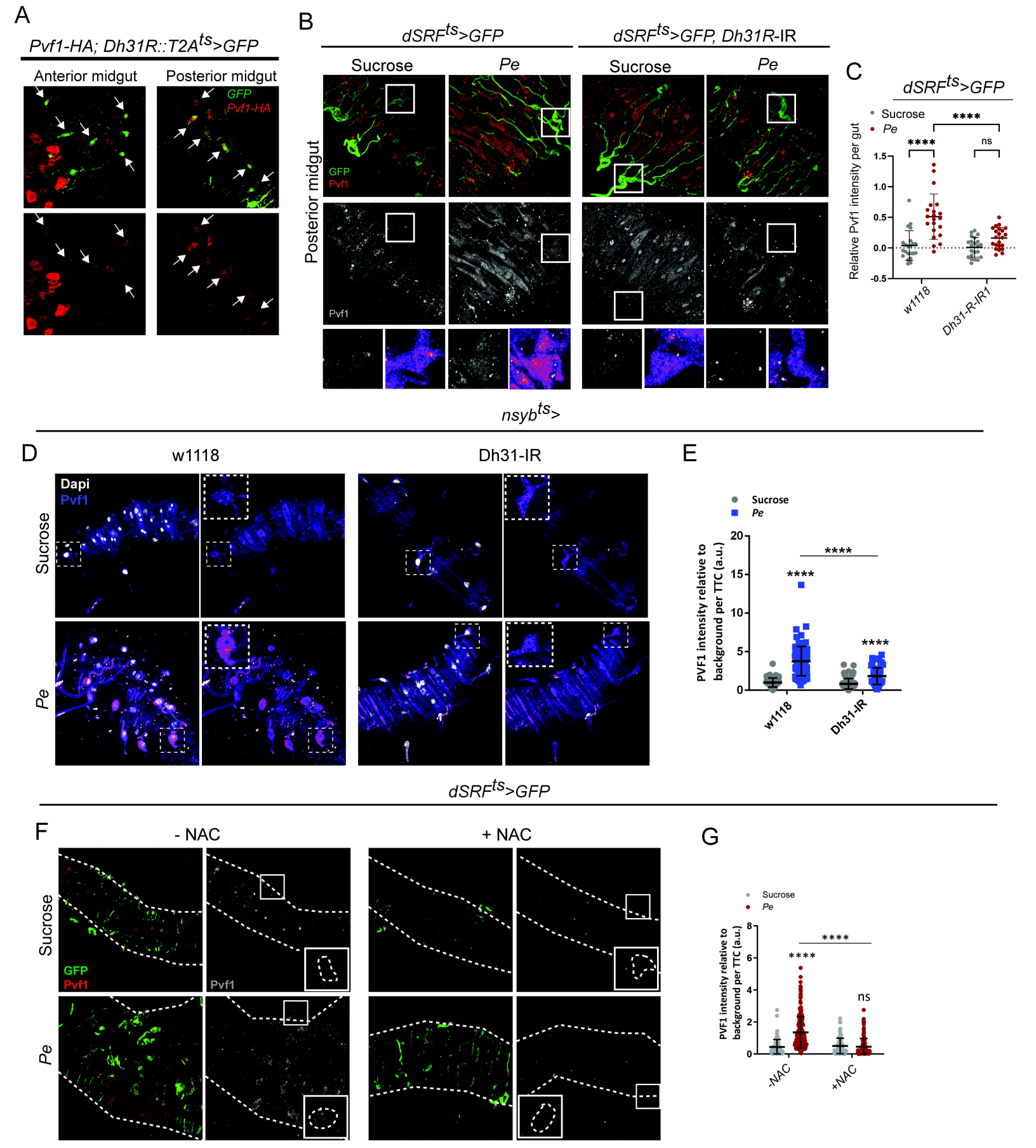
A
Pvf1-HA; Dh31R::T2A^ts>GFP
Anterior midgut
Posterior midgut
GFP
Pvf1-HA
B
dSRF^ts>GFP
dSRF^ts>GFP, Dh31R-IR
Sucrose
Pe
Sucrose
Pe
Posterior midgut
GFP
Pvf1
Pvf1
C
dSRF^ts>GFP
Sucrose
Pe
****
****
ns
Relative Pvf1 intensity per gut
1.5
1.0
0.5
0.0
-0.5
w1118
Dh31-R-IR1
nsyb^ts>
D
w1118
Dh31-IR
Dapi
Pvf1
Sucrose
Pe
E
Sucrose
Pe
PVF1 intensity relative to background per TTC (a.u.)
20
15
10
5
0
****
****
****
w1118
Dh31-IR
dSRF^ts>GFP
F
- NAC
+ NAC
Sucrose
Pe
GFP
Pvf1
Pvf1
G
Sucrose
Pe
PVF1 intensity relative to background per TTC (a.u.)
8
6
4
2
0
****
****
ns
-NAC
+NAC